Supplementary Figure 1 (a-b) HAADF images of initial f-phase before and after electron beam irradiation which last about 15-20 min. No obvious vacancy ordering layer formed after the irradiation except for some unclear damage area indicated by red ellipse. (b-d) HAADF images of vacancy ordering f-phase before and after electron beam irradiation which last about 15-20 min. No obvious shift for the vacancy ordering layer after the irradiation except for some unclear damage area by red ellipse. Scale bar, (a-d) 1 nm.

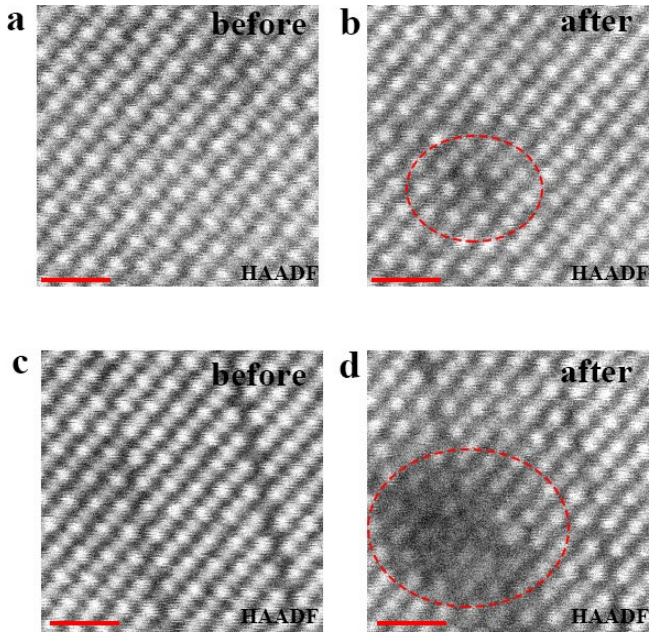

Supplementary Figure 2 (a) HAADF image of an intermediate f-phase. **(b-g)** The comparison between no filter and filter atomic EDS mapping figures taken from image (a). The inset of each image is the FFT pattern extracted from the corresponding element, in which all of the diffraction spots in each of b-d are contained correspondingly in each of e-g, indicating that all of the structural information in each of b-d is contained correspondingly in each of e-g. Scale bar, (a-g) 1 nm.

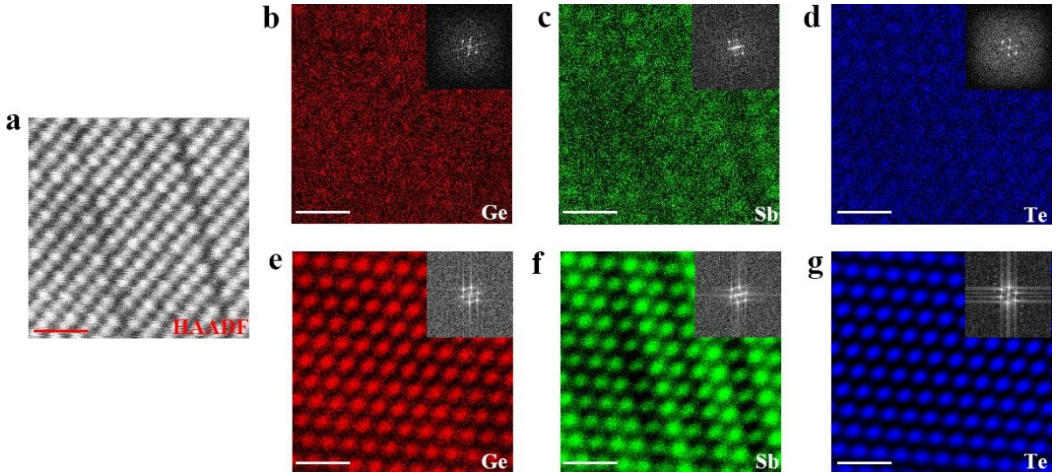

Supplementary Figure 3 A typical atomic EDS mapping of cubic perovskite $SrTiO_3$ sample processed with wiener filting. **(a)** The HAADF image of $SrTiO_3$ projected along [100] orientation, which shows a periodical contrast-intensity fluctuation owing to incoherent scattering intrinsic. **(b-d)** The atomic mapping pictures of Sr, Ti and O atoms, respectively. The obtained atomic result quite fits well with the atomic model. This was used to test and optimise the instrument parameter when conducting atomic EDS mapping experiment. The sample preparation process is the same as $Ge_2Sb_2Te_5$ films by using FIB technique with standard lift out and polishing process in FEI Helios 600 instrument and cleaning in Gatan 691 PIPS at 0.8 keV. Scale bar, (a-d) 0.5 nm.

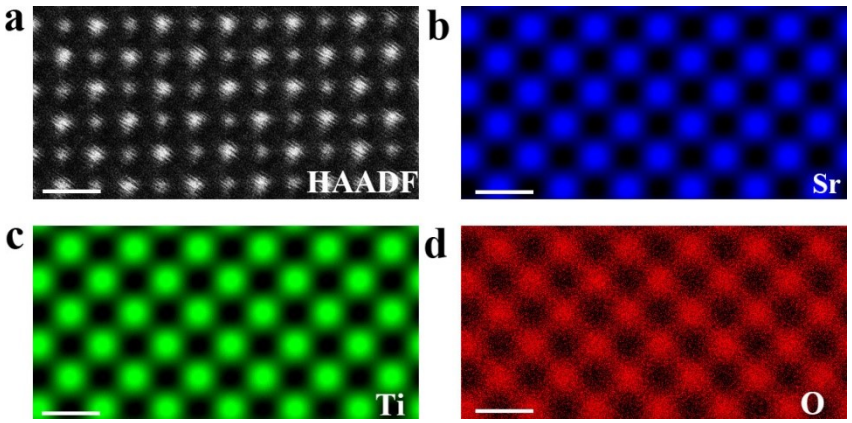

Supplementary Figure 4 (a-c) The overlay atomic EDS mapping results of every two elements by pairs taken from area 2. **(d)** The overlay atomic EDS mapping results of three elements. According to (a-d), it is clear that Ge and Sb atoms occupy cationic sites, and Te atoms occupy anionic sites in the initial i-phase. Scale bar, (a-d) 1 nm.

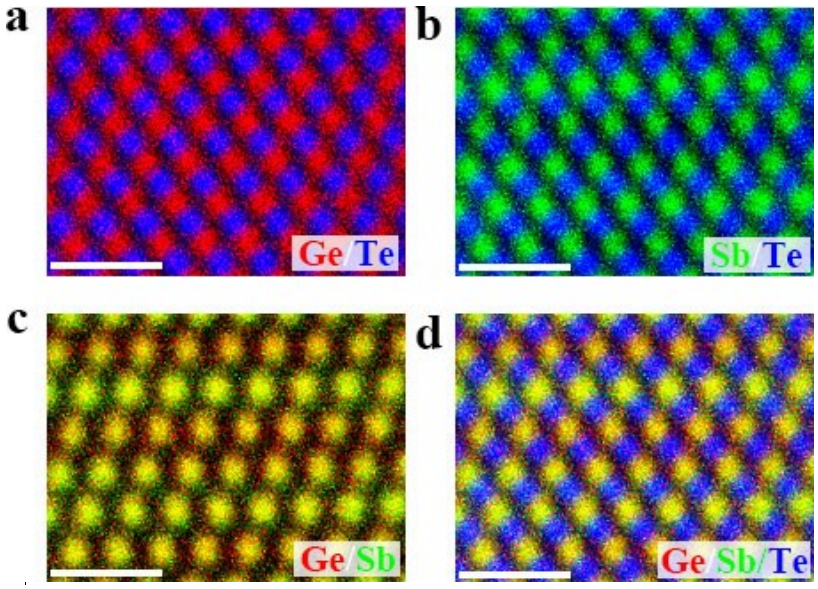

Supplementary Figure 5 (a-c) The overlay atomic EDS mapping results of every two elements by pairs taken from area 3. **(d)** The overlay atomic EDS mapping results of three elements. According to (a-d), Ge and Sb atoms still occupy cationic sites, and Te atoms occupy anionic sites in the deeper migration i-phase. Scale bar, (a-d) 1 nm.

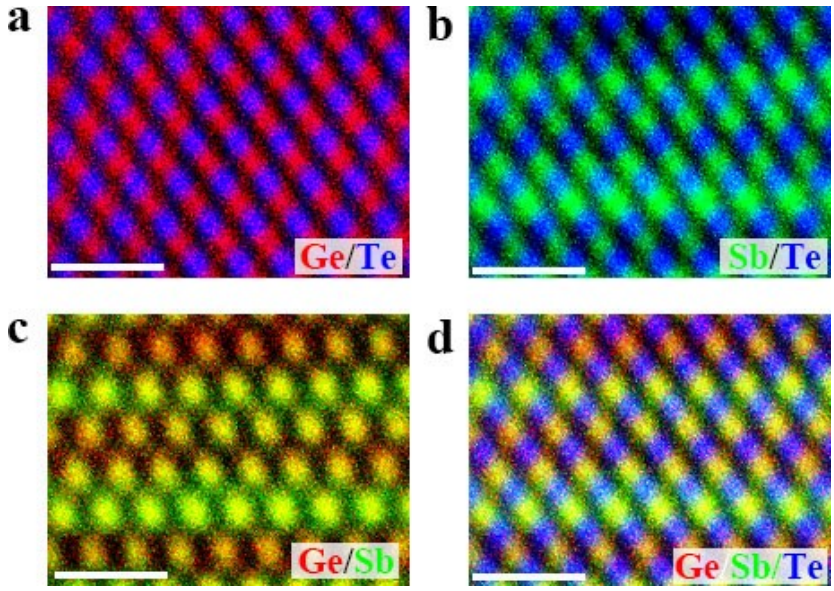

Supplementary Figure 6 (a-c) The overlay atomic EDS mapping results of every two elements by pairs taken from area 4. According to (a-c), Ge and Sb atoms still occupy cationic sites, and Te atoms occupy anionic sites in the further deeper migration i-phase. Scale bar, (a-c) 1 nm.

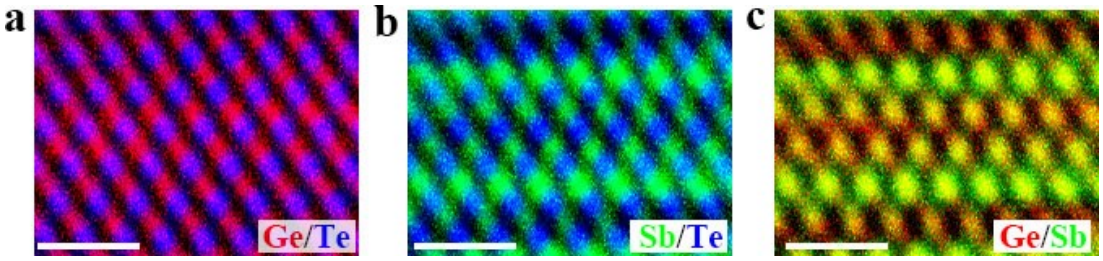

Supplementary Figure 7 (a-c) The overlay atomic EDS mapping results of every two elements by pairs taken from h-phase. According to (a-c), we can find that in h-phase, Ge and Sb atoms still occupy cationic sites, and Te atoms occupy anionic sites. **(d)** The overlay atomic EDS mapping results of three elements taken from h-phase. Labels 2-5 on the left side refer to the cationic Ge/Sb layers, in which EDS raw data will be extracted as indicated by the dashed white rectangles. Labels a-i on the right side refer to the anionic Te columns or cationic Ge/Sb columns, in which EDS raw data will be extracted as indicated by the open white circles. Scale bar, (a-d) 1 nm.

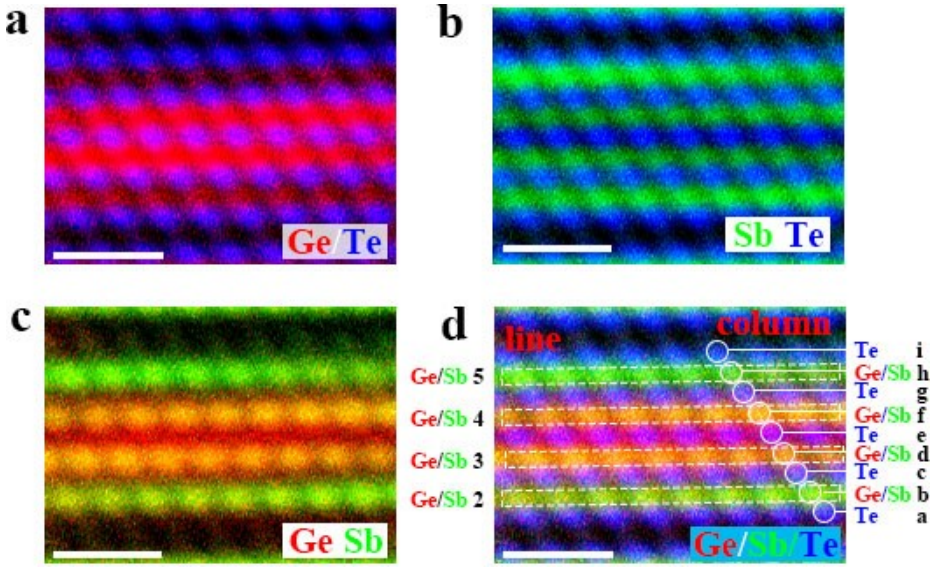

Supplementary Note 1

Though atomic resolution mapping has been successfully utilized to qualitatively analyze the atomic migration behavior of cationic atoms during the f-to-h phase transition, it would be significantly complicated to conduct quantitative analysis for the concentration detail in each cationic site for Ge and Sb elements. Accounting for the elastic and thermal scattering of the electron probe, there is a substantial contribution to all signals from columns which do not contain the element in question[1]. Supplementary Table 1 depicts the EDS raw counts of three elements in different columns extracted from the blocks as denoted in Supplementary Figure 7(d). It is clearly found that every atomic column has signal of three elements, which obstructs the directly absolute analysis of three elements. Though Ge, Sb and Te elements show different signal levels that relate to the factors such as fluorescence yields, x-ray absorption, and detector geometry[2,3,4], we can still find that the variation signal phenomenon reflecting the location for cationic and anionic sites as shown in Supplementary Figure 8. From the raw counts data, we can see the occupation trend of cation, that is, Ge element prefers the inner cationic layers and Sb element likes the outer cationic layers in the blocks.

Supplementary Table 1 EDS raw data for Ge, Sb and Te elements in different columns. Raw data were extracted from the open white circles areas as depicted in Supplementary Figure 7.

Column		Ge (counts)	Sb (counts)	Te (counts)
Te	a	25.3	73.67	242.9
Ge/Sb	b	51.99	160.32	225.36
Te	c	21.19	82.09	247.26
Ge/Sb	d	72.6	128.57	194.22
Te	e	18.37	95.42	249.22
Ge/Sb	f	53.04	112.82	176.48
Te	g	36.04	69.04	238.83
Ge/Sb	h	46.19	161.16	167.72
Te	i	33.53	97.72	230.33

Supplementary Figure 8 The counts distributions in different columns in the 9 layers building block in stable h-phase extracted from the EDS raw data in Supplementary Table 1.

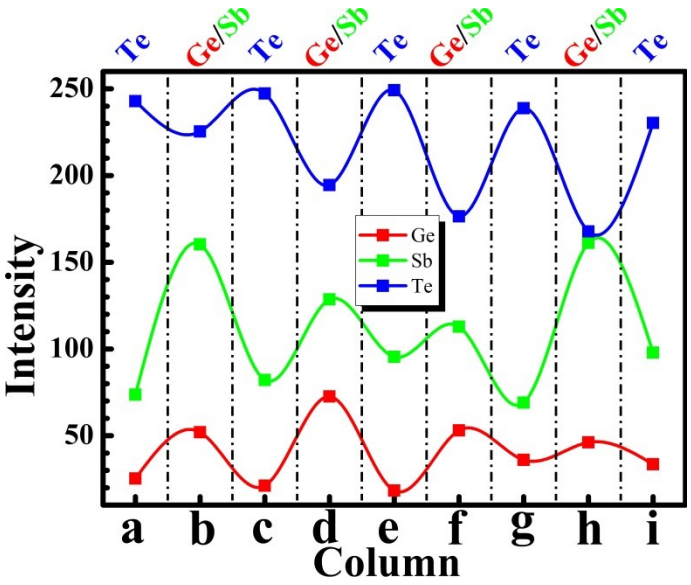

Supplementary Note 2

To achieve a preliminary understanding of the cationic distribution in h-phase, the EDS raw data collected from different cationic layers and columns in Supplementary Figure 7(d) were summarized in Supplementary Table 2 and Table 3. Considering that only some smears of Ge and Sb elements reside in Van der Waals gap as seen in Supplementary Figure 7, it's reasonable to assume that the majority of Ge and Sb atoms have migrated into the blocks. Then, we utilize the formula $X_{i\text{-}Nor.}=X_i/\sum_{i=2}^{5} X_i$ *(X=Ge, Sb)* to acquire a reliable concentrate of Ge and Sb elements in different cationic layers. Since the atomic percent of Ge and Sb is nearly the same in the GST alloy, we can compare the atomic distribution of Ge and Sb in the 9 layers block by using the formula $(Ge/Sb)_i=Ge_{i\text{-}Nor.}/Sb_{i\text{-}Nor}$. Regardless of the intrinsic defects from the electron probe, which make it much complicate to get the exact Ge/Sb ratio in each layer, Supplementary Table 2 and Table 3 both reveal that Ge element prefers the inner cationic layers and Sb element prefers the outer cationic layers in the blocks.

Supplementary Table 2 EDS raw data for Ge, Sb and Te elements in different cationic layers. Raw data were extracted from the dashed white rectangles as depicted in Supplementary Figure 7.

Layer	Ge (counts)	$Ge_{Nor.}$	Sb (counts)	$Sb_{Nor.}$	Ge/Sb (ratio)
Ge/Sb (line2)	1639.7	0.251	4381.6	0.267	0.94
Ge/Sb (line3)	1843.3	0.282	3726.4	0.227	1.24
Ge/Sb (line4)	1653.5	0.253	3717.5	0.227	1.12
Ge/Sb (line5)	1389.9	0.213	4573.1	0.279	0.76

Supplementary Table 3 EDS raw data for Ge, Sb and Te elements in different cationic columns. Raw data were extracted from the open white circles areas as depicted in Supplementary Figure 7.

Column	Ge (counts)	$Ge_{Nor.}$	Sb (counts)	$Sb_{Nor.}$	Ge/Sb (ratio)
Ge/Sb b	51.99	0.232	160.32	0.285	0.81
Ge/Sb d	72.6	0.324	128.57	0.228	1.42
Ge/Sb f	53.04	0.237	112.82	0.200	1.18
Ge/Sb h	46.19	0.206	161.16	0.286	0.72

Supplementary References

1. Kothleiner, G. *et al*. Quantitative elemental mapping at atomic resolution using X-ray spectroscopy. *Phys. Rev. Lett.* **112**, 085501 (2014).
2. Wang, J.-J. *et al*. Genesis and effects of swapping bilayers in hexagonal $GeSb_2Te_4$. *Chem. Mater.* **30**, 4770-4777 (2018).
3. Watanabe, M. & Williams, D. B. The quantitative analysis of thin specimens: a review of progress from the Cliff-Lorimer to the new ζ-factor methods. *J. Microsc.* **221**, 89-109 (2006).
4. Kotula, P. G., Klenov, D. O. & Harrach, H. S. Challenges to quantitative multivariate statistical analysis of atomic-resolution X-ray spectral. *Microsc. Microanal.* **18**, 691-698 (2012).